



Temporal shifts in the abundance and preferred habitats of yellowfin and bigeye tuna larvae in the Gulf of Mexico

Maëlle Cornic^{a,*}, Jay R. Rooker^{a,b}

^a Department of Marine Biology, Texas A&M University (Galveston Campus), 1001 Texas Clipper Road, Galveston, TX 77554, USA

^b Department of Wildlife and Fisheries Sciences, Texas A&M University, College Station, TX 77843, USA

ARTICLE INFO

Keywords:

Habitat suitability models
Distribution and abundance
Tuna larvae
Cyclonic and anticyclonic features
Gulf of Mexico

ABSTRACT

The influence of environmental conditions on the relative abundance of *Thunnus albacares* (yellowfin tuna) and *Thunnus obesus* (bigeye tuna) were investigated to determine the extent of the early life stage suitable habitat of these species in the Gulf of Mexico (GoM). *Thunnus albacares* and *T. obesus* larvae were commonly found (31–50% frequency of occurrence per year) in the northern GoM (26–28°N, 91–96°W), and a significant intra- and inter-annual variability in abundance of *T. albacares* and *T. obesus* was observed with higher abundance recorded in July surveys (1.3 larvae 1000 m⁻³ for both species) and during the Summer 2009 (1.9 and 1.7 larvae 1000 m⁻³, respectively). Generalized additive models (GAMs) indicated that larvae of *T. albacares* and *T. obesus* were more common and at higher abundance in water masses with moderate to high salinity (28–36), high temperature (29 °C), positive sea surface height. Species-specific environmental preferences determined with GAMs were then combined with summer environmental data over eight years (2007 to 2015) to predict the spatial coverage of suitable habitat of both species in regions beyond the 100-m isobath. Habitat suitability predictions indicated that the location and extent of highly suitable habitat of *T. albacares* and *T. obesus* larvae varied across years with the highest areal coverage in 2015 (70%) and 2010 (73%), respectively. Both *T. albacares* and *T. obesus* larvae were more commonly observed and at higher abundance off the continental slope and at margins of the Loop Current and associated warm-core eddies in the northern GoM. Because changes in environmental conditions influenced the spatio-temporal distribution of *T. albacares* and *T. obesus* larvae, habitat suitability models are valuable tools for identifying critical areas of the GoM inhabited by tuna larvae and this information can also be used to assess potential impacts of natural and anthropogenic disturbances on the recruitment and population dynamics of tunas.

1. Introduction

The quality of spawning and nursery habitats of pelagic fishes (e.g. billfishes, tunas) is known to influence their population dynamics (Lehodey et al., 2006; Hare, 2014), and changes in environmental conditions can affect both early life survival and recruitment (Pepin, 1991; Lehodey et al., 2003; Kimura et al., 2010). Therefore, it is essential to determine habitat associations of pelagic fishes during early life as well as identify oceanographic conditions that define suitable nursery areas. Habitat-modeling approaches have been used in recent years to link the spatiotemporal distribution of pelagic fish larvae with environmental conditions to assess fish-habitat relationships and evaluate the potential impacts of habitat changes (Muhling et al., 2011; Rooker et al., 2013). These modeling approaches also have been used to identify

the location of key production (spawning) and nursery zones of several taxa of pelagic fishes (Reglero et al., 2014; Mourato et al., 2014; Alvarez-Berastegui et al., 2016).

True tunas (genus *Thunnus*) represent a significant source of food worldwide and support important commercial fisheries due to their high economical value. Despite management plans to ensure the long-term sustainability of tuna stocks in the Atlantic Ocean, including the Gulf of Mexico (GoM), several species or stocks are considered to be overfished (ICCAT, 2019). In the GoM, *T. thynnus* (Atlantic bluefin tuna), *T. albacares* (yellowfin tuna), and *T. obesus* (bigeye tuna) represent important components of commercial fisheries, and management plans for these species are based primarily on fisheries-dependent catch data from commercial operations (ICCAT, 2019). While fisheries-dependent data provide wide spatial coverage, preferential sampling due to

* Corresponding author.

E-mail address: cornicmaelle@yahoo.fr (M. Cornic).

<https://doi.org/10.1016/j.jmarsys.2021.103524>

Received 27 May 2020; Received in revised form 10 January 2021; Accepted 2 February 2021

Available online 17 February 2021

0924-7963/© 2021 Elsevier B.V. All rights reserved.

commercial constraints (specific species, size, and areas) can bias predicted distributions and population estimates (Fromentin and Powers, 2005; Maunder and Piner, 2014). Moreover, the relationship between recruit and spawner biomass is often used to predict the productivity of fish stock. This spawner-recruit relationship is generally uncertain because environmental factors affecting spawner biomass and the development of early life stages until recruitment are largely ignored in fisheries management (Skern-Mauritzen et al., 2016). Environmental conditions of the spawning and nursery grounds experienced by the early life stages of tunas may impact their growth and survival (Lang et al., 1994; García et al., 2013; Reglero et al., 2014), and in turn, the recruitment success of tuna stocks. Because recruitment success may explain the dynamics of tuna populations and ultimately influence the status of the stock (Alvarez-Berastegui et al., 2018), a better understanding of critical early life stages of tuna is needed in the GoM.

Fisheries-independent indices of larval abundance have proven useful for assessing the population dynamics of *T. thynnus* in the GoM (Ingram et al., 2010; Muhling et al., 2010, 2011; Domingues et al., 2016). Comparable indices for other true tunas are rare even though this region is known to be an important spawning area for congeners, including *T. albacares* and *T. obesus*. Both of these tropical tunas are assumed to spawn into the GoM, but the location and coverage of spawning and/or larval nursery areas for these species is uncertain (Reglero et al., 2014). To date, information on distribution and abundance of *T. albacares* and *T. obesus* larvae in the GoM is incomplete, and the distribution of both species during early life is assumed to be highly variable due to dynamic nature of mesoscale oceanographic features (Loop Current and eddies) and riverine discharges from the Mississippi-Atchafalaya River System (MARS) (Lang et al., 1994; Lindo-Atichati et al., 2012). These factors likely influence the quality of nursery habitats experienced by *T. albacares* and *T. obesus* larvae, which in turn will affect their survival and population dynamics.

Here, we evaluated how the natural and induced disturbances (i.e. oceanographic conditions, oil spill) affect the spatial and temporal distribution of *T. albacares* and *T. obesus* larvae in the northern GoM. Because misidentification of *Thunnus* larvae can compromise efforts to characterize spatial distributions of these species (Puncher et al., 2015), a genetic approach was applied to identify species within the Genus *Thunnus* to develop species-specific habitat suitability models.

2. Method

2.1. Sampling and data collection

Pelagic fishes including true tunas are known to spawn in the GoM during the summer. Surveys were conducted in June and July 2007 to 2009 to coincided with summer spawning in areas of the outer shelf and slope where true tuna larvae are widely distributed (Lindo-Atichati et al., 2012; Reglero et al., 2014). We collected *T. albacares* and *T. obesus* from surface waters using two neuston nets each with a 1 m × 2 m rectangular opening and two different mesh sizes (500- μ m and 1200- μ m). General Oceanic flowmeters were mounted in the center of the mouth of each net to measure the volume of water filtered. Nets were towed at an average depth of 0.8 m during daytime for 10 min to an approximate speed of 2.5 knots. Stations were spaced every 15 km to sample various oceanographic features, and all fish larvae were preserved on board in 95% ethanol.

2.2. Larval identification

In the laboratory, each *Thunnus* larva was visually identified to genus level using morphological and pigmentation characters (Richards, 2006) and preserved in 70% ethanol. Small *Thunnus* larvae are difficult to visually identify to the species level due to similar pigmentation. Consequently, *Thunnus* larvae were genetically identified using a highly sensitive genotyping method, high-resolution melting analysis (HRMA)

using an unlabeled probe, following the protocol described in Cornic et al. (2018). During the three sampling years, a high number of *Thunnus* larvae ($N = 15,573$) were collected. In response, a subset of 163 positive stations (nearly 50% of stations containing *Thunnus* larvae) was selected for further analysis. Because *Thunnus* larvae at several positive stations were present in high numbers (>100), we randomly selected 100 individuals at these stations for HRMA. The percent composition of *T. albacares* and *T. obesus* from the 100 larvae was used to assign species identification to the remainder of the *Thunnus* larvae in the sample. At stations with less than 100 individuals, all the larvae were identified with HRMA to the species level. Moreover, each larva genetically identified was measured to the nearest 0.1 mm from the tip of the snout to the tip of the notochord using the software Image-Pro Plus 7.0.

2.3. Environmental data

Sea surface temperature and salinity were recorded on board at each station from 2007 to 2009 using a YSI Sonde 6920 Environmental Monitoring System (YSI, Inc). For each survey, supplementary environmental data (chlorophyll *a* concentration, sea surface height) were downloaded and extracted from remotely sensed observations using station coordinates and date of sampling. All other environmental data used to predict habitat suitability from 2007 to 2015 were extracted from remotely sensed observations (Table 1). For habitat models, temperature and salinity were determined using Gulf of Mexico Hybrid Coordinate Ocean Model (GoM-HYCOM 31.0) added to U.S. Navy Coupled Ocean Data Assimilation (NCODA) system. Because in situ measurements were used to develop habitat models and remotely sensed observations were used for predictions of habitat suitability in subsequent years to 2015, correlation between both sources of data was calculated to determine if GoM-HYCOM observations reflect the values collected during ichthyoplankton surveys (2007–2009). Sea surface temperatures from both data sources were highly correlated ($r = 0.8$), while salinity had a lower rate of correlation ($r = 0.2$). This lack of correlation between in situ and GoM-HYCOM observations, it is most likely due to the difference of temporal and spatial scales between measurements. Riverine inputs rapidly alter the salinity seascape in the GoM, and HYCOM models may not accurately capture these changes at spatial and temporal fine-scales. However, HYCOM is well defined to detect changes in salinity over a longer period of time (Cummings and Smedstad, 2014). Therefore, changes in salinity (low, intermediate, high) will be reflected in the predictions and GoM-HYCOM values are still a good proxy to determine the influence of salinity changes on *T. albacares* and *T. obesus* larvae distribution. All remotely sensed environmental data were extracted using the marine geospatial ecology toolbox in ArcGIS 10.2 (Roberts et al., 2010).

2.4. Data analysis

Ichthyoplankton surveys conducted before the Deepwater Horizon oil spill (2007–2009) were considered as baseline surveys and used to develop habitat models. Because *Thunnus* larvae are often distributed

Table 1

Source and spatial resolution of remotely data sensed extracted to predict suitable habitat of *Thunnus albacares* larvae (yellowfin tuna) and *Thunnus obesus* larvae (bigeye tuna).

Variables	Source	Link	Spatial resolution	Temporal resolution
Sea surface temperature (°C)	GoM-HYCOM+NCODA	www.hycom.org	0.04°	1 month
Salinity (psu)				
Sea surface height (m)	AVISO	www.aviso.oceano.org	0.25°	1 month

throughout the epipelagic zone (0–200 m), it was important to investigate if the surface sampling performed with neuston nets impacted *T. albacares* and *T. obesus* collections. Abundance of *T. albacares* and *T. obesus* from neuston net tows (1200- μm mesh size) in the upper meter of the water column were compared to abundance from oblique bongo tows (paired nets: 333- μm and 500- μm mesh size) in the water column to 100 m in 2011, 2012, and 2015 surveys (Fig. 1). Neuston net and bongo net tows were performed simultaneously during the daytime, and mean abundance of *T. albacares* and *T. obesus* were typically higher in bongo net than neuston net, although a significant difference in abundance was only detected for *T. albacares* (paired *t*-test, $p < 0.05$). *T. albacares* was detected in higher abundance in the 500- μm mesh size neuston net, this mesh size was not used in 2011, 2012 and 2015, which might explain that the abundance between the bongo and neuston nets were significantly different for this species. Nevertheless, matching bongo and neuston tows (either both nets with or both nets without tuna larvae) occurred at 85% of the stations for *T. albacares* and 74% of the stations for *T. obesus*, suggesting that our characterizations of distribution and abundance from surface sampling effectively captured spatial variation in the occurrence and abundance of *T. albacares* and *T. obesus* in the epipelagic zone.

The spatial distribution of *T. albacares* and *T. obesus* from 2007 to 2009 was examined by visualizing the abundance of each species in our sampling corridor using ArcGIS 10.2. Variation in larval abundance among years and between months was investigated using the aligned rank transform (ART) for non-parametric factorial ANOVA test using the package ARTool in R (Wobbrock et al., 2011; R Development Core Team, 2017). Interaction analysis in package phia (De Rosario-Martinez, 2015) was used to evaluate the statistical significance of differences observed between months and among years.

Baseline ichthyoplankton cruises (2007–2009) were used to investigate the potential distribution of *T. albacares* and *T. obesus* from 2007 to 2015. Two-stage generalized additive models or GAMs were developed to explore the influence of environmental conditions on the distribution and abundance of *T. albacares* and *T. obesus* (Barry and Welsh, 2002; Grüss et al., 2014). Use of two-stage GAMs involves independently developing an occurrence-based GAMs (presence-absence) and an abundance-based GAMs (presence only). The first stage of the analysis is to model the occurrence of *T. albacares* and *T. obesus* using binomial distribution and a logit link function. In the second stage, abundance-based GAMs were developed using a quasipoisson distribution and a log link function. The total number of individuals collected for each species was pooled between both neuston nets (500- μm , 1200- μm) for calculation of occurrence (presence = 1 and absence = 0) and

standardized abundance (larvae 1000 m^{-3}). Net (mesh size) was also included as factor in the model to take into account the potential influence of 500- μm and 1200- μm mesh size neuston net on *Thunnus* larvae collection (Fig. 2). Explanatory variables used to develop GAMs were salinity, sea surface temperature, sea surface height, chlorophyll *a*, distance to the Loop Current, Mississippi river discharge and depth. To reduce the instability of the model the multicollinearity between explanatory variables was investigated using variance inflation factor (VIF) and Spearman's correlation test. Explanatory variables with VIF > 5 and/or a Spearman's correlation >0.6 were considered as highly collinear. Multicollinearity tests indicated that chlorophyll *a* concentration and salinity, Mississippi River discharge and SST, depth and distance to the Loop Current were collinear. To determine the most influential variable for occurrence and abundance-based GAMs, each variable was tested in separate models and the variable that resulted in the lowest Akaike information criterion (AIC) or quasi Akaike information criterion (QAIC) value was included in the initial model. Consequently, chlorophyll *a* concentration, Mississippi River discharge and distance to the Loop Current were removed from our models. All models were built with cubic regression splines restricted to 4 degrees of freedom to avoid over-parametrization using the mgcv package (Wood, 2015) in R 3.4.0 (R Development Core Team, 2017). To select the explanatory variables influencing the occurrence and abundance of *T. albacares* and *T. obesus* larvae, a dredge function was used to generate all possible models and model selection was made by comparing AIC, Akaike weight, and logLik. Models with ΔAIC less than 2 were considered as good models (Richards, 2005). If the competitive models were similar and the likelihood was not improving when a more complex model was built, the simple model was kept as best model (Leroux, 2018). The weight of each explanatory variable in the final model was determined by removing each explanatory variable from the final model and calculating the change in percent deviance explained (ΔDE) and AIC or QAIC (ΔAIC , ΔQAIC) between each model (Rooker et al., 2012).

Final GAMs and environmental conditions in 2007 to 2015 were used to predict *T. albacares* and *T. obesus* larvae distribution in the northern GoM. The grid points (cell size = 0.0833°) used to extract the environmental data in 2007 to 2015 were linked to a prediction grid using predict.gam function in the mgcv package in R (Wood, 2015). Then, the predicted occurrence and abundance were combined (combined model) for each location sampled (Barry and Welsh, 2002). Combined predictions of occurrence and abundance of *T. albacares* and *T. obesus* larvae from 2007 to 2015 were smoothed using bilinear interpolation to visualize their suitable habitats. Predicted values of zero were assumed to represent unsuitable habitat and maximum values an optimal habitat

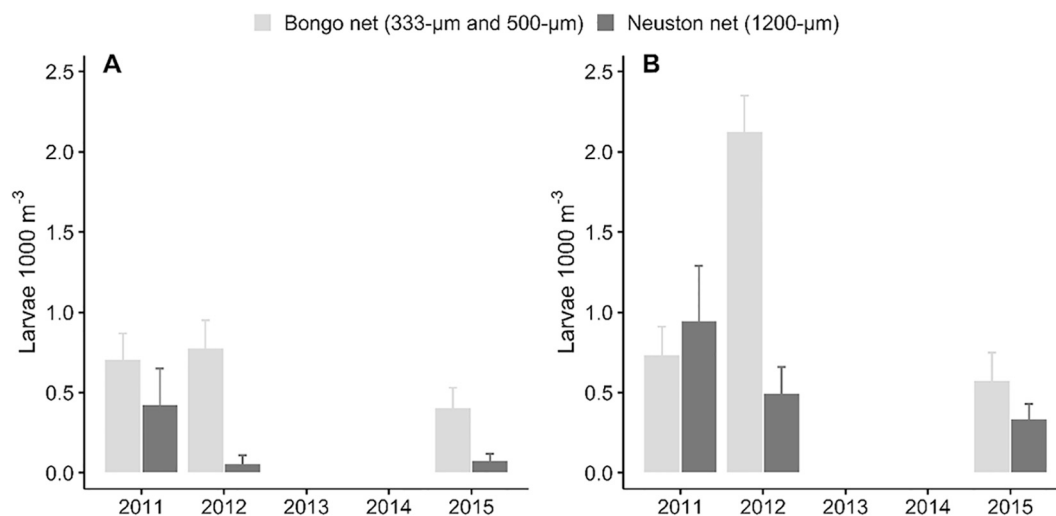


Fig. 1. Comparison in larval abundance for A) *Thunnus albacares* (yellowfin tuna) and B) *Thunnus obesus* (bigeye tuna) between neuston net (1200- μm) and bongo nets (333- μm and 500- μm) in the northern Gulf of Mexico. Error bars represent the standard error of the mean.

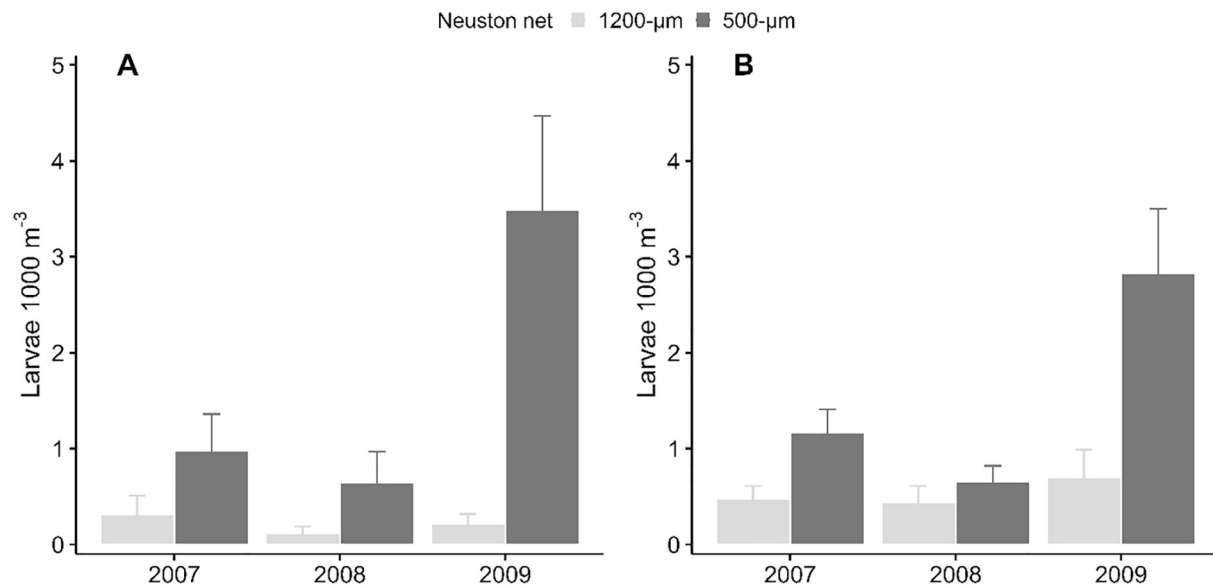


Fig. 2. Comparison in larval abundance for *Thunnus albacares* (yellowfin tuna) and *Thunnus obesus* (bigeye tuna) between 1200- μm mesh size and 500- μm mesh size neuston net in the northern Gulf of Mexico. Error bars represent the standard error of the mean.

corresponding to areas with favorable oceanographic conditions to support the survival of larvae in this region. Given that the mean abundance of *T. albacares* and *T. obesus* from 2007 to 2009 was 1 larva 1000 m⁻³, highly suitable habitat of both species in this study was defined as predicted values greater than 1 larva 1000 m⁻³. Subsequently from 2007 to 2015 when these habitats were detected, the areal coverage of highly suitable habitat was estimated using ArcGis 10.2. Further analysis was performed in 2010 to investigate the impact of the Deepwater Horizon (DWH) oil spill on distribution of *T. albacares* and *T. obesus*. The maximum DWH oil spill coverage was estimated by cumulating the oil spill area from June to July 2010. Then, the area of highly suitable habitat impacted by the oil spill was calculated by overlapping the maximum DWH oil spill coverage on distribution maps of *T. albacares* and *T. obesus*.

The predictive capability of the occurrence and combined models (2007–2009) was evaluated by applying a range of evaluation statistics (discrimination power, correlation and calibration statistics). To assess the performance of the baseline models, 80% of the dataset was randomly selected to build the models (number stations = 174) and predict the remaining 20%. Then, discrimination power analysis on occurrence models were performed to assess the ability of the models to discriminate the presence and absence of species (Pearce and Ferrier, 2000). Discrimination was tested using a receiver operating characteristic (ROC) curves and the area under the curve (AUC) (package pROC; Robin et al., 2011). AUC value lower than 0.5 indicates that the predictions are not better than random and an AUC value of 1 represents a perfect discrimination between presence and absence. An AUC value between 0.7 and 0.9 is considered as a reasonable discrimination and values higher than 0.9 are excellent discrimination (Pearce and Ferrier, 2000).

The level of agreement between predictions and observations in the combined models were also investigated (Potts and Elith, 2006). Similarity in magnitude and order of the predictions in relation to observations were tested using the Spearman's rank correlation coefficient (ρ). Spearman's rank correlation represents the similarity between the ranks of the predicted and observed values. The calibration model was assessed by a linear regression (observed = $m(\text{predicted}) + b$) and provides information for the bias and consistency of the predictions. In the equation, m represents an indication of the spread of predictions compare to the spread of the observations of model prediction and b represents an indication of the bias of the model. Finally, we examined

the predictive ability of the model using forecasting accuracy measures: root mean square error (RMSE) and mean error (ME).

3. Results

3.1. Catch summary

A total of 341 *T. albacares* and 378 *T. obesus* larvae were genetically identified, and these larvae represented 7% and 8% of all *Thunnus* larvae identified at the 163 positive stations ($N = 4901$); *T. atlanticus* (blackfin tuna) were numerically dominant in our samples, accounting for 83% of the *Thunnus* larvae in our collections. *T. albacares* and *T. obesus* larvae ranged in size from 2.0 to 8.2 mm in total length (Fig. 3). A higher proportion of smaller *T. albacares* was observed relative to *T. obesus*; however, larvae of both species were of similar size in June and July with a majority of *T. albacares* ranging from 2.0 to 5.0 mm (88%) and a majority of *T. obesus* ranging from 5.0 to 7.0 mm (79%). *T. albacares* and *T. obesus* were common in our sampling corridor with a percent frequency of occurrence ranging among years from 15 to 41% and 33 to 65%, respectively. Intra- and inter-annual variability in abundance was observed for *T. albacares* and *T. obesus* (Fig. 3), with mean abundance lower in June than July for *T. albacares* (0.51 ± 0.21 and 1.33 ± 0.36 larvae 1000 m⁻³) and *T. obesus* (0.50 ± 0.17 and 1.35 ± 0.31 larvae 1000 m⁻³). A difference in mean abundance among years was also detected with a maximum abundance of both *T. albacares* and *T. obesus* observed in 2009 (1.91 ± 0.54 and 1.71 ± 0.23 larvae 1000 m⁻³, respectively) and the lowest mean abundance for each detected in 2008 (0.31 ± 0.54 and 0.46 ± 0.17 larvae 1000 m⁻³, respectively).

Both *T. albacares* and *T. obesus* were mostly distributed on the continental slope (depth = 200 to 2000 m) (Fig. 4); however, *T. albacares* was also common in areas of the northern GoM influenced by the freshwater inputs from the Mississippi River. *T. albacares* and *T. obesus* densities were typically higher on the margin of the Loop Current and associated eddies, and maximum abundance recorded during our survey occurred at stations close to the edge of these mesoscale features. Stations far removed from the Loop Current or the absence of mesoscale features within a survey (i.e., limited northward penetration of the Loop Current) generally resulted in lower abundance for both species (Fig. 4).

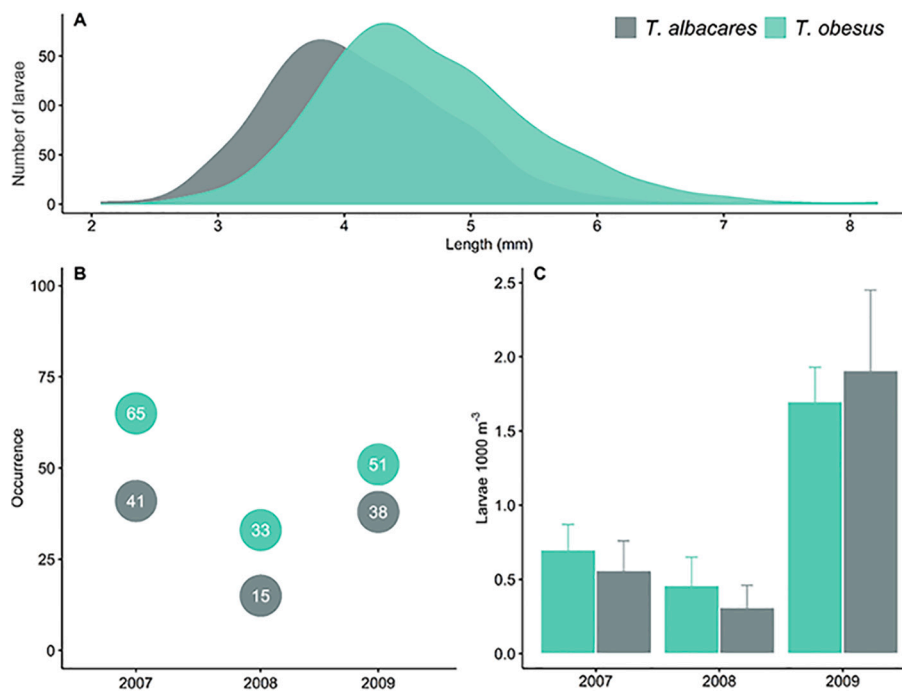


Fig. 3. Size frequency (A), percent frequency of occurrence (B), and larval abundance with error bars representing the standard error of the mean (C) of *Thunnus albacares* (yellowfin tuna) and *Thunnus obesus* (bigeye tuna) from 2007 to 2009.

3.2. Habitat models

Occurrence-based (AIC = 377.8, DE = 16.8%) and abundance-based (QAIC = 74.1, DE = 44.7%) GAMs for *T. albacares* included sea surface height, salinity, and sea surface temperature (Table 2). Based on Δ AIC and Δ DE (%), salinity was the most influential environmental variables retained in the final occurrence-based GAM (5.6, 1.0%) and abundance-based GAM (4.3, 8.4%). Response plots for occurrence- and abundance-based GAMs indicated (Fig. 5) that the presence and abundance of *T. albacares* larvae were higher at intermediate to high salinity (30–36), at negative and positive sea surface heights (–10 to 10 cm), and at higher sea surface temperatures (>29 °C).

Occurrence-based (AIC = 538.5, DE = 10.2%) and abundance-based GAM (QAIC = 160.2, DE = 58.4%) GAMs for *T. obesus* included three similar variables: salinity, sea surface height, and sea surface temperature (Table 3). Based on Δ AIC and Δ DE (%), salinity was the most influential variable retained in occurrence-based GAM (10.2, 3.1%) and sea surface temperature in the abundance-based GAM (55.0, 23.0%). Response plots for occurrence- and abundance-based GAMs (Fig. 6) showed that *T. obesus* larvae were most likely observed at intermediate to high salinity (31–36), at negative and positive sea surface heights (–20 to 20 cm), and at higher sea surface temperatures (> 30 °C).

3.3. Suitable habitat predictions

Proportion of suitable habitat of *T. albacares* and *T. obesus* larvae was estimated from 2007 to 2015 in the northern GoM using the combined model predictions (Table 4; Figs. 7, 8), and areas deemed to be suitable for *T. albacares* were more constrained (mean 174,329 km²) than *T. obesus* (mean 205,958 km²). Distributions of suitable habitat for *T. albacares* larvae (>100 m isobath) from 2007 to 2015 were mostly confined to the outer continental shelf (depth < 200 m) but extended across the entire northern GoM in most years. In contrast, suitable habitat of *T. obesus* was predicted to occur primarily in the eastern and the central regions of the northern GoM in 2007 to 2008, while from 2009 to 2015 suitable habitat occurred primarily in continental shelf and slope waters (depth < 2000 m) with additional suitable areas in the

western GoM. The areal coverage of highly suitable habitat (defined as >1 larva 1000 m⁻³) of both species was highly variable among the years examined ranging from 5% (2007) to 70% (2015) for *T. albacares* and 11% (2007) to 73% (2010) for *T. obesus*. Moreover, highly suitable habitat of *T. albacares* and *T. obesus* affected by the Deepwater Horizon oil spill in 2010 was relatively modest with 17% and 18% of the high value habitat exposed to surface oil, respectively.

Habitat suitability maps generated for *T. albacares* and *T. obesus* were related to observed abundance from ichthyoplankton surveys performed in 2007 to 2009 (Figs. 7, 8). For both species, highly suitable habitat determined by the models corresponded to areas where the highest abundance were observed, indicating that *T. albacares* and *T. obesus* were distributed at the margin of the Loop Current and areas potentially impacted by the riverine inputs (28°N, 89°W). Moreover, year with highest mean densities (2009) corresponded to the highest percent of highly suitable habitat observed (31 and 72%), while years of lower mean densities (2007–2008) the percent of highly suitable habitat was variable with 5 to 22% for *T. albacares* and 11 to 48% for *T. obesus*.

3.4. Model validation

Discrimination power of occurrence models were evaluated using ROC curves to assess model fit (Table 4). The AUC values show that the predictions performed better for *T. albacares* (AUC > 0.70; $r = 0.34$) than *T. obesus* (AUC > 0.65; $r = 0.22$). This is reflected in the greater percent of correct prediction for absence and presence for *T. albacares* (72%) than *T. obesus* (64%).

Calibration statistics were performed on the combined models (Table 5); therefore, predicted abundance was the product of predicted probability of presence and predicted abundance. Combined models for *T. albacares* and *T. obesus* explained 30% and 27% of the variation in abundance. The rank correlation between observed and predicted values was slightly dissimilar ($\rho = 0.40$ – 0.32 ; $p < 0.01$) and predictive performance of the combined model for *T. obesus* was more accurate than *T. albacares* with a lower error around predictions, a lower bias. Also, the spread of the predicted values was similar to the spread of the observed values (Table 5). Still, bias and range of prediction compared to the

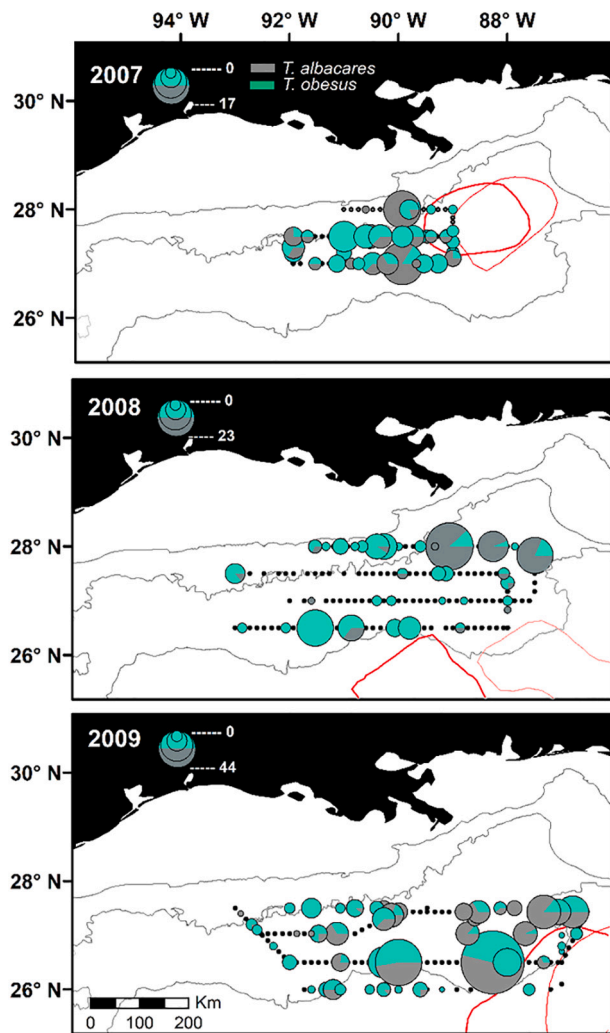


Fig. 4. Proportional abundance (larvae 1000 m^{-3}) of *Thunnus albacares* (yellowfin tuna) and *Thunnus obesus* (bigeye tuna) in the northern Gulf of Mexico from 2007 to 2009. Circles represent the total abundance of *T. albacares* and *T. obesus* for each station. Note that the proportional abundance of each species varies among years. Red lines represent the margin of anticyclonic features (warm-core eddy and/or the Loop Current) in June (thin line) and in July (thick line). Grey lines are 100 m, 1000 m, 3000 m isobaths. (For interpretation of the references to colour in this figure legend, the reader is referred to the web version of this article.)

observations were small for *T. albacares* indicating that predictive performance of combined models for both species were reliable to predict abundance.

4. Discussion

The presence of *T. albacares* and *T. obesus* larvae throughout our sampling corridor (31% and 50% frequency of occurrence; 0.98 and 1.05 larvae 1000 m^{-3}) indicates that the northern GoM is likely a spawning habitat of both species, and possibly an important larval nursery habitat. Previously, the GoM was defined as a key spawning area for *T. thynnus* (Muhling et al., 2010, 2012; Reglero et al., 2014) and it has been demonstrated that mean abundance during daytime of *T. thynnus* ranged from 0.005 larvae 1000 m^{-3} (neuston net) to 0.05 larvae 1000 m^{-3} (10–20 m, MOCNESS net) in this region (Habtes et al., 2014). Despite the potential bias associated with comparisons of different types of sampling methods between Habtes et al. (2014) and the present study, mean larval abundance of *T. albacares* and *T. obesus*

Table 2

Akaike information criterion (AIC), Quasi Akaike information criterion (QAIC), deviance explained (DE) and variables retained in the final occurrence- and abundance-based generalized additive models for *Thunnus albacares* larvae (yellowfin tuna). Variation in AIC (ΔAIC), QAIC (ΔQAIC), DE (ΔDE), and p values ($***p < 0.001$, $**p < 0.01$, and $*p < 0.05$) are also presented to evaluate the importance of each variable.

	Variable	DE	AIC/ QAIC	ΔDE	$\Delta\text{AIC}/$ ΔQAIC
Occurrence	Salinity*	15.8	383.4	1.0	5.6
	Sea surface height*	15.5	382.3	1.3	4.5
	Sea surface temperature*	16.1	379.5	0.7	1.7
	Net***	8.2	412.9	8.6	35.1
Abundance	Salinity*	36.3	78.4	8.4	4.3
	Sea surface height	43.3	72.3	1.4	-1.8
	Sea surface temperature*	36.5	78.0	8.2	3.9
	Net*	39.2	77.2	5.5	3.1

were much higher (0.98 ± 0.21 and 1.05 ± 0.17 larvae 1000 m^{-3}) than *T. thynnus* supporting the notion that the northern GoM is a valuable spawning area for both *T. albacares* and *T. obesus*. Oceanographic conditions in the GoM are influenced by the seasonal penetration of the Loop Current and its associated eddies, and this likely affects the distribution of *Thunnus* larvae, and possibly the delivery of larvae from the southern GoM (via Yucatan Channel) into the northern GoM (Quian et al., 2015). However, the presence of numerous recently hatched larvae in our samples (<3 mm or < 4 days old; age approximated from Lang et al., 1994) suggest that most of these individuals were likely from spawning events in the northern GoM. Although high abundance of *Thunnus* larvae in our samples supports the presumed value of the GoM as spawning habitat, this region might not provide suitable conditions for larval growth and survival. Previous study comparing the growth of *Thunnus* larvae in the GoM with others spawning grounds in the Straits of Florida and Mediterranean Sea demonstrated that the growth of *Thunnus* larvae was faster in the GoM (Malca et al., 2017). Because a large body size can positively affect the survival of *Thunnus* larvae (Satoh et al., 2013), the faster development of *Thunnus* larvae in the GoM indicates that this region likely represents a favorable early life habitat for *T. albacares* and *T. obesus*. While spawning events of *T. albacares* were previously reported in the GoM (Lang et al., 1994; Richardson et al., 2010), this region has not been yet described as a potential spawning area for *T. obesus* because larvae are not often observed in this area (Richards et al., 1990; Richardson et al., 2010). Our results lend further support to the premise that the northern GoM represents a potentially overlooked and important spawning area for both *T. albacares* and *T. obesus*.

The distribution and abundance of *Thunnus* larvae in the northern GoM are not fixed in space or time, and vary both within and across years (Lindo-Atichati et al., 2012; Cornic et al., 2018). Intra- and inter-annual variation in the occurrence of larvae observed in our study may be explained by changes in the geographic position of mesoscale features in this region, including the Loop Current (Richardson et al., 2010; Rooker et al., 2012; Lindo-Atichati et al., 2012; Kitchens and Rooker, 2014; Randall et al., 2015). Observed variation in abundance of both *T. albacares* and *T. obesus* was related to the proximity of the station to the margin of the Loop Current or associated eddies, and mean abundance for both *T. albacares* and *T. obesus* larvae was highest in 2009 and 2007 (1.91 ± 0.54 and 1.71 ± 0.23 larvae 1000 m^{-3}), years of significant northward penetration of the Loop Current or when strongly defined warm-core eddies were present in our sampling corridor. In contrast, during the year with the lowest northward penetration of the Loop Current (2008), abundance of *T. albacares* and *T. obesus* were lower (0.31 ± 0.15 and 0.46 ± 0.19 larvae 1000 m^{-3}). Therefore, the geographic position of this mesoscale feature most likely influences the

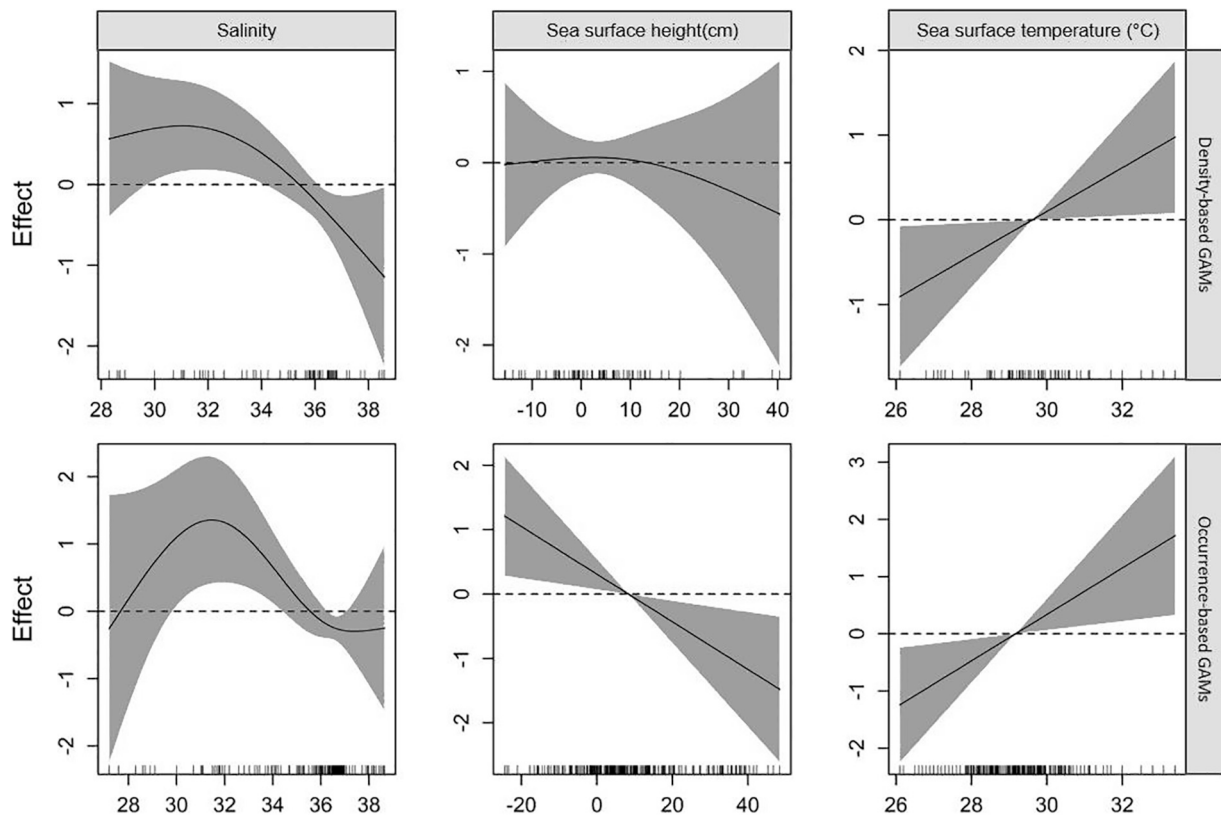


Fig. 5. Response plots of occurrence-based and abundance-based generalized additive models showing the effects of environmental data on *Thunnus albacares* larvae (yellowfin tuna). Variable retained were sea surface temperature, sea surface height anomaly, and salinity. Positive effect corresponds to an increase of occurrence and abundance while a negative effect corresponds to a decrease. Shaded areas represent 95% confidence intervals and black lines along the x-axis represent the number of observations.

Table 3

Akaike information criterion (AIC), Quasi Akaike information criterion (QAIC), deviance explained (DE) and variables retained in the final occurrence- and abundance-based generalized additive models for *Thunnus obesus* larvae (bigeye tuna). Variation in AIC (Δ AIC), QAIC (Δ QAIC), DE (Δ DE), and p values (** $p < 0.001$, * $p < 0.01$, and $p < 0.05$) are also presented to evaluate the importance of each variable.

	Variable	DE	QAIC	Δ DE	Δ AIC/ Δ QAIC
Occurrence DE = 10.2% QAIC = 538.5	Salinity*	7.1	548.7	3.1	10.2
	Sea surface height	8.7	543.2	1.5	5.3
	Sea surface temperature*	8.9	541.8	1.3	3.3
	Net***	4.6	568.6	5.6	30.0
Abundance DE = 58.4% AIC = 160.2	Salinity***	46.9	185.0	11.5	24.8
	Sea surface height*	53.3	168.4	5.1	8.2
	Sea surface temperature***	35.4	215.2	23.0	55.0
	Net**	55.4	166.3	3.0	6.1

distribution and abundance of both *T. albacares* and *T. obesus* larvae. Our findings are consistent with results of previous studies showing that the abundance of pelagic fish larvae often increases near anticyclonic or warm-core oceanographic features (Richardson et al., 2010; Reglero et al., 2014; Domingues et al., 2016).

Variability in the spatiotemporal distribution patterns of *T. albacares* and *T. obesus* larvae also can be linked to the hydrodynamic processes and biological production associated with oceanographic features. In the GoM, hydrodynamic processes at the margin of mesoscale features generate convergent zones that aggregate planktonic organisms and increase productivity (Govoni and Grimes, 1992; Bakun, 2006; Greer

et al., 2020). Our models showed that occurrence and abundance of *T. albacares* and *T. obesus* increased at sampling stations proximal to mesoscale feature, suggesting that hydrodynamic processes affect the distribution and abundance of these species. Alternatively, the concentration of zooplankton in convergent zones can produce high spatial overlap between fish larvae and their prey (Schmid et al., 2020). Because mechanisms that concentrate prey of fish larvae (e.g., cladocerans, copepods) play a role in feeding success of *Thunnus* larvae (Llopiz and Hobday, 2015), increased availability of prey in the convergent zones might result in faster growth and survival of *T. albacares* and *T. obesus*. Since the GoM is an oligotrophic environment, convergent zones at the margin of the mesoscale features may offer a favorable habitat for *T. albacares* and *T. obesus* larvae by retaining and transporting *Thunnus* larvae along with productive water masses.

Physicochemical conditions such as temperature and sea surface height are known to affect habitat associations of pelagic fishes during early life (Wexler et al., 2011; Reglero et al., 2014; Kim et al., 2015; Dell’Apa et al., 2018) and both were also influential in explaining the distribution and abundance of *Thunnus* larvae in the present study. The Loop Current and its associated cold- and warm-core eddies influence sea surface temperatures in the GoM. *T. albacares* and *T. obesus* larvae were detected over a wide range of sea surface temperature (26–33 °C) and different mesoscale features (negative and positive SSH). Although our models predicted high occurrence and abundance of *T. albacares* and *T. obesus* larvae in areas with higher sea surface temperatures (>29 °C), no clear relationship was observed between larval distribution and SSH. Both species were frequently encountered at stations with both negative and positive SSH; however, high abundances were predominantly detected at stations within positive SSH. *Thunnus* larvae are often observed in warm waters which most likely coincides to the temperature requirement for their development and survival (Wexler et al., 2011;

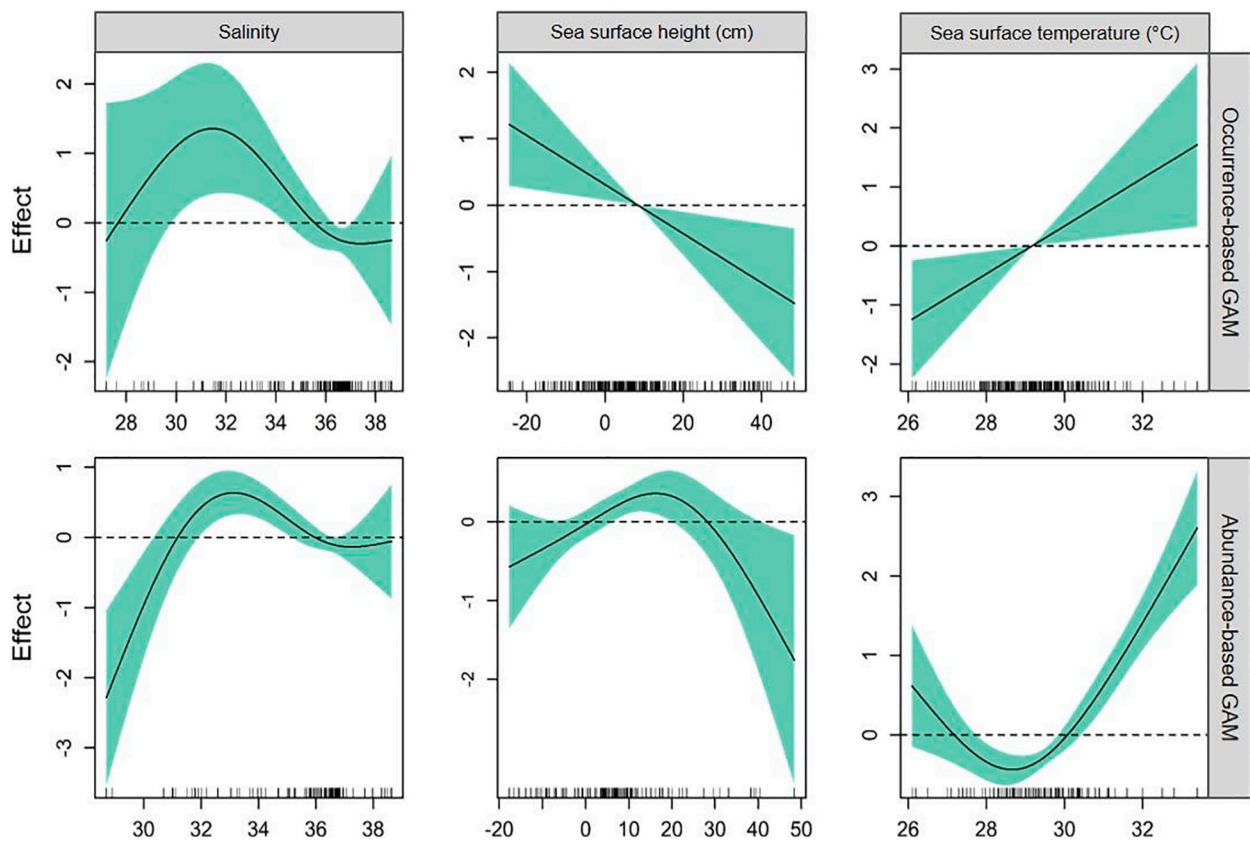


Fig. 6. Response plots of occurrence-based and abundance-based generalized additive models showing the effects of environmental data on *Thunnus obesus* larvae (bigeye tuna). Variable retained were sea surface temperature, sea surface height anomaly, and salinity. Positive effect corresponds to an increase of occurrence and abundance while a negative effect corresponds to a decrease. Shaded areas represent 95% confidence intervals and black lines along the x-axis represent the number of observations.

Table 4

Model validation for occurrence models of *Thunnus albacares* larvae (yellowfin tuna) and *Thunnus obesus* larvae (bigeye tuna). Area under the curve (AUC), the Spearman's coefficient (ρ) and percentage of correct predicted presence and absence are presented.

	AUC	ρ	% Correct presence	% Correct absence
<i>T. albacares</i>	0.75	0.38	0.66	0.78
<i>T. obesus</i>	0.65	0.18	0.65	0.64

Dell'Apa et al., 2018; Reglero et al., 2018). While studies on *T. obesus* larvae are scarce, it has been demonstrated that growth of *T. albacares* larvae is positively linked to temperature with higher growth rates at elevated temperature between 28 and 31 °C (Lang et al., 1994; Wexler et al., 2011). Therefore, warm-core features might represent more suitable habitat for faster growth and possibly higher survival of *T. albacares* and *T. obesus*, which can influence the abundance of both species. Similar results worldwide were observed indicating that the distribution of several tuna species, including *T. albacares* and *T. obesus* larvae, was correlated to mesoscale activities and higher temperatures (Reglero et al., 2014; Domingues et al., 2016; Hernández et al., 2019). These results support that warm-core features and open-ocean regions of the GoM may represent a more suitable habitat than cold-core eddies, further emphasizing the importance of oceanographic features on the spatial extent of suitable habitat of these species.

Another important physicochemical factor that affected the distribution and abundance of *Thunnus* larvae was salinity, which is influenced by spatial and temporal dynamics of the Mississippi-Atchafalaya River System (MARS) in the northern GoM (Lang et al., 1994; Muhling et al., 2010; Lindo-Atichati et al., 2012). The amount of riverine

discharge can affect the spatial distribution of low salinity waters and primary productivity in the northern GoM, with MARS inflow occasionally reaching the outer continental shelf (Amon and Benner, 1998; Androulidakis et al., 2019). *T. albacares* and *T. obesus* were found in a wide range of salinities (28–36), indicating that these species may be tolerant of conditions observed throughout the northern GoM. Still, peaks in presence and abundance of *T. albacares* and *T. obesus* were observed at intermediate salinities (32–34), which corresponds to areas impacted by MARS discharges (Androulidakis et al., 2019). Because the growth and survival of *Thunnus* larvae are dependent on food availability (Llopiz et al., 2010; Llopiz and Hobday, 2015), areas of higher productivity and lower salinity might correspond to the optimal conditions for *T. albacares* and *T. obesus* larvae. This hypothesis is further supported by a previous study showing that *T. albacares* larvae were influenced by MARS discharges in this region, with higher larval abundance and growth rates near the river plume (Lang et al., 1994). In the present study, high abundance of *T. albacares* and *T. obesus* were observed in 2009, which was a year of increased MARS discharges (780,802 ft³ sec⁻¹) compared to 2007 and 2008 (460,431 and 612,214 ft³ sec⁻¹) (USACE, www.mvn.usace.army.mil). Therefore, the magnitude of riverine discharges appears to influence the distribution and abundance of both species by modifying the physicochemical conditions of the northern GoM.

Habitat models predicted that *T. albacares* and *T. obesus* larvae were associated with the Loop Current and warm-core eddies with higher abundance at the margin of these features. The geographical location of the Loop Current in this region vary seasonally and annually which may explain the dynamic nature of the highly suitable habitat for both species predicted over the eight years. However, there are many factors that have a potential to affect the highly suitable habitat of each species (i.e.

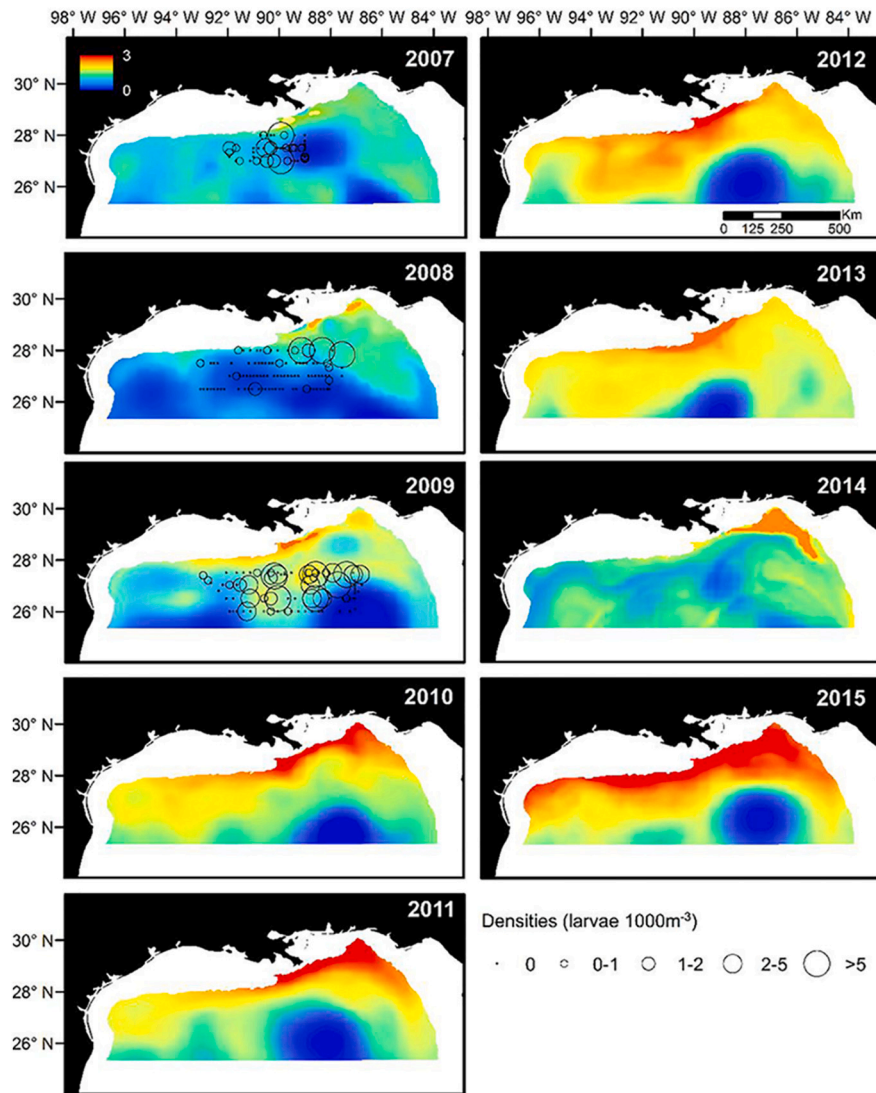


Fig. 7. Predictive maps of *Thunnus albacares* larvae (yellowfin tuna) distribution based on environmental data of each year from 2007 to 2015, and species-specific environmental preferences from generalized additive models (2007–2009). Black circles represent abundance observed (larvae 1000 m⁻³) during ichthyoplankton cruises.

growth rates, prey concentration). High abundance of tuna larvae can potentially increase predation and competition and in turn, affect the growth and survival of *Thunnus* larvae (Bakun, 2006; Reglero et al., 2011; Satoh et al., 2013). Because convergence zones might aggregate *Thunnus* larvae in high abundance patches, these zones might not be always suitable for *T. albacares* and *T. obesus* larvae. While including more biological factors would help to better define the extent of highly suitable habitat of *T. albacares* and *T. obesus* larvae, oceanographic features have been shown as major predictors influencing the distribution of *Thunnus* larvae. This suggests that oceanographic conditions are robust predictors to detect shift in distribution of *T. albacares* and *T. obesus* larvae in the northern GoM. Moreover, suitable habitat of *Thunnus* larvae can be affected by pollution (Hazen et al., 2016; Gove et al., 2019). In 2010 the Deepwater Horizon (DWH) incident discharged the largest oil spill observed in pelagic environment (>4 million barrels), impacting the spawning ground of tunas and other pelagic fishes in the northern GoM (Muhling et al., 2012; Rooker et al., 2013). It has been observed that abundance of *Thunnus* larvae in the northern GoM decreased the summer following the DWH oil spill (Cornic et al., 2018), which is not unexpected given that crude oil has been shown to reduce the survival of tuna larvae (Incardona et al., 2014; Brette et al., 2014). In this study, predictions of highly suitable habitats for *T. albacares* and

T. obesus indicated that larvae were distributed close to, or within, the surface oil slick associated with the DWH event. Nevertheless, a large fraction of the predicted highly suitable habitat of *T. albacares* and *T. obesus* in 2010 was observed to occur in eastern and western regions of the northern GoM in areas apparently unaffected by the oil spill, which might explain the relatively low percent of suitable habitat exposed to surface oil (17 and 18%). While exposure to surface oil may have affected larval survival following the DWH event and may possibly explain lower observed abundance for both species in 2010, the estimated percent coverage of suitable habitat of *T. albacares* and *T. obesus* larvae affected by the oil spill was relatively modest. Our results are consistent with other studies investigating the impact of the DWH event on tuna spawning and larval nursery habitat (Muhling et al., 2012; Rooker et al., 2013; Hazen et al., 2016). While DWH event might have a direct impact and explain the decline in abundance in 2010, the impact of DWH event may have been mitigated to some degree by the large amount of suitable habitat still available in the northern GoM, suggesting that observed differences in the distribution and abundance of *T. albacares* and *T. obesus* in 2010 may be due to other factors such as the more limited northward penetration of the Loop Current (Rooker et al., 2013).

Given that the quality of spawning and larval nursery habitat is

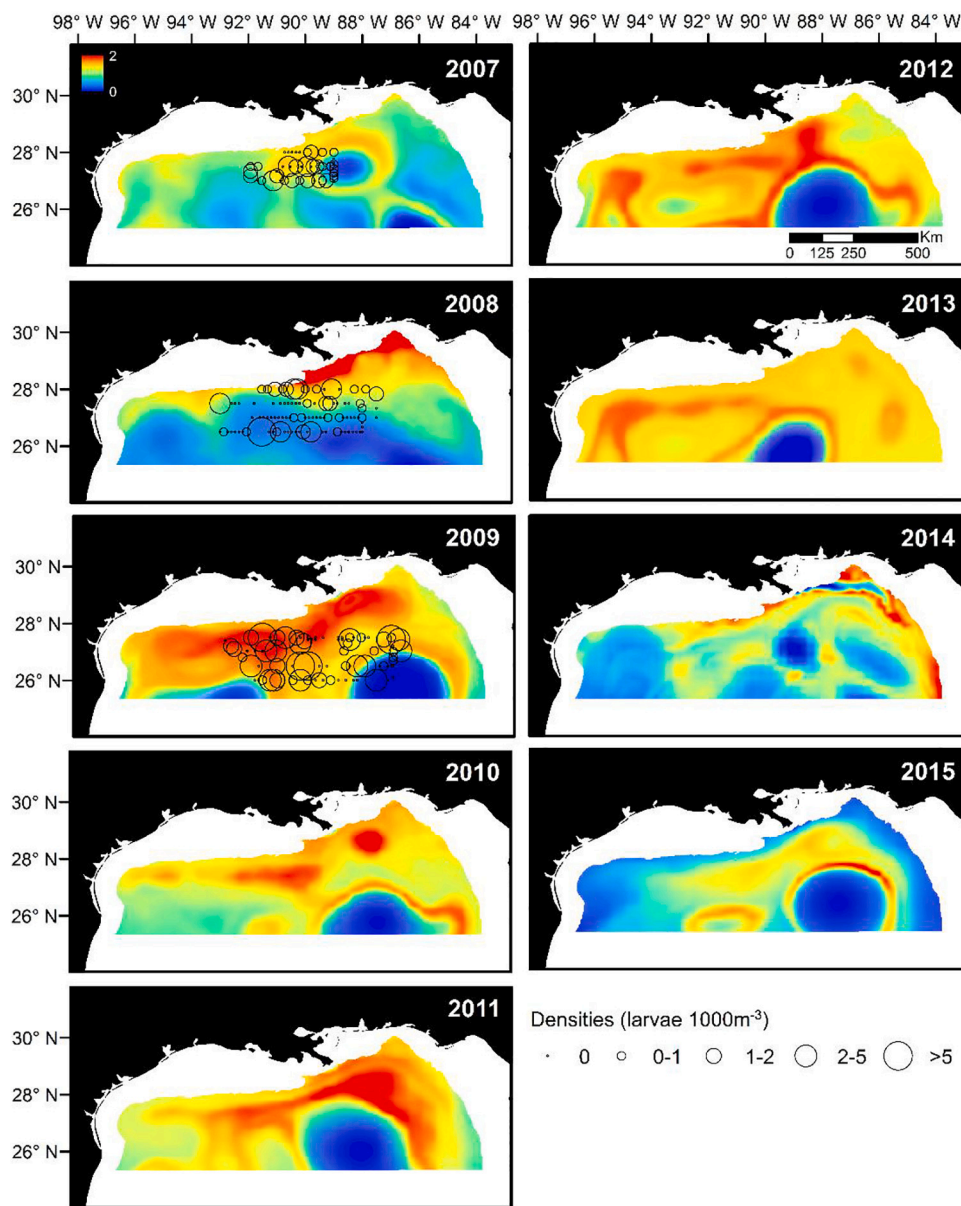


Fig. 8. Predictive maps of *Thunnus obesus* larvae (bigeye tuna) distribution based on environmental data of each year from 2007 to 2015, and species-specific environmental preferences from generalized additive models (2007–2009). Black circles represent abundance observed (larvae 1000 m⁻³) during ichthyoplankton cruises.

Table 5

Model performance statistics for combined models of *Thunnus albacares* larvae (yellowfin tuna) and *Thunnus obesus* larvae (bigeye tuna). ρ is the Spearman’s rank coefficient, calibration: observed = $m(\text{predicted}) + b$, RMSE is the root mean square error, ME is the mean of error.

	Correlation	Calibration		Error indices		
	Spearman’s (ρ)	Intercept (m)	Slope (b)	R ²	RMSE	ME
<i>T. albacares</i>	0.40	0.64	0.14	0.27	2.45	1.09
<i>T. obesus</i>	0.32	0.93	0.05	0.30	1.62	0.97

critical for the survival and recruitment of *Thunnus* in the GoM (Lehodey et al., 2003; Muhling et al., 2010; Rooker et al., 2013; Dell’Apa et al., 2018), it is important to determine the potential effect of habitat degradation on larval abundance. Habitat quality of *T. albacares* and *T. obesus* was predicted by our models with areas characterized as

suitable for both species (e.g., margin of the Loop Current, convergent zones) corresponding to highest densities observed in our sampling corridor from 2007 to 2009. It is also important to note that elevated occurrence and abundance of larvae were predicted to occur at the edge of the projected area (~100-m isobath along the shelf edge), suggesting that the distribution of *T. albacares* and *T. obesus* might be broader and extend onto the continental shelf. Therefore, it is essential to estimate the occurrence and the abundance of *T. albacares* and *T. obesus* larvae in regions outside the sampling area of this study to predict more precisely their suitable habitat in the northern GoM.

5. Conclusion

Summer ichthyoplankton surveys combined with genetic identification (HRMA) revealed that *T. albacares* and *T. obesus* were commonly found in the northern Gulf of Mexico (GoM), suggesting that this region may represent valuable spawning and/or larval nursery habitat for these species. Our findings indicated that several physicochemical conditions

were influential in the spatial distribution of *T. albacares* and *T. obesus*. Highly suitable habitats of both species were characterized by moderate to high salinity (28–36), sea surface temperatures above (29 °C) and close proximity to fronts associated with mesoscale oceanographic features Loop Current and warm-core eddies and the MARS discharges. Although suitable habitats of *T. albacares* and *T. obesus* larvae were affected by the DWH oil spill, the impact of this event remains unclear due to the dynamic nature of physicochemical and oceanographic conditions that govern the location and extent of highly suitable habitats of both species. Because abundance of larvae may influence the recruitment success of tunas, our results provide essential information to better understand recruitment variability in space and time, and its relative contribution to tuna population changes. This information is essential to improve the predictability in population dynamics which may reduce the uncertainty in stock assessment and management advice.

Declaration of Competing Interest

None.

Acknowledgements

We thank the reviewers for their helpful comments. A special thanks to members of the Fisheries Ecology Lab and the Marine Ecology and Fisheries Genetics Lab for their support during the ichthyoplankton cruises and assistance with molecular identification of larvae. This work was supported by grants from the McDaniel Charitable Foundation, Louisiana State University, and the Louisiana Department of Wildlife and Fisheries.

References

- Alvarez-Berastegui, D., Hidalgo, M., Tugores, M., Reglero, P., Aparicio-González, A., Cianelli, L., Juza, M., Mourre, B., Pascual, A., López-Jurado, J., García, A., Rodríguez, J., Tintoré, J., Alemany, F., 2016. Pelagic seascape ecology for operational fisheries oceanography: Modelling and predicting spawning distribution of Atlantic bluefin tuna in Western Mediterranean. *ICES J. Mar. Sci.* 73, 1851–1862.
- Alvarez-Berastegui, D., Saber, S., Ingram Jr., G.W., Díaz-Barroso, L., Reglero, P., Macías, D., García-Barcelona, S., Ortiz de Urbina, J., Tintoré, J., Alemany, F., 2018. Integrating reproductive ecology, early life dynamics and mesoscale oceanography to improve albacore tuna assessment in the Western Mediterranean. *Fish. Res.* 208, 329–338.
- Amon, R.M.W., Benner, R., 1998. Seasonal patterns of bacterial abundance and production in the Mississippi River plume and their importance for the fate of enhanced primary production. *Microb. Ecol.* 35, 289–300.
- Androulidakis, Y., Kourafalou, V., Le Hénaff, M., Kang, H.S., Sutton, T., Chen, S., Hu, C., Ntaganou, N., 2019. Offshore spreading of Mississippi waters: pathways and vertical structure under eddy influence. *J. Geophys. Res. Oceans.* 124, 5952–5978.
- Bakun, A., 2006. Fronts and eddies as key structures in the habitat of marine fish larvae: opportunity, adaptive response and competitive advantage. *Sci. Mar.* 70, 105–122.
- Barry, S.C., Welsh, A.H., 2002. Generalized additive modeling and zeroinflated count data. *Ecol. Model.* 157, 179–188.
- Brette, F., Machado, B., Cros, C., Incardona, J.P., Scholz, N.L., Block, B.A., 2014. Crude oil impairs cardiac excitation-contraction coupling in fish. *Science* 343, 772–776.
- Cornic, M., Smith, B.L., Kitchens, L.L., Alvarado Bremer, J.R., Rooker, J.R., 2018. Distribution and habitat associations of tuna larvae in the northern Gulf of Mexico. *Hydrobiologia* 806, 29–46.
- Cummings, J.A., Smedstad, O.M., 2014. Ocean data impacts in global HYCOM. *J. Atmos. Ocean. Technol.* 31, 1771–1791.
- De Rosario-Martinez, H., 2015. *phia*: post-hoc interaction analysis. In: R package version 0.1-3. Available. <http://CRAN.R-project.org/package=phia>.
- Dell’Apa, A., Carney, K., Davenport, T.M., Carle, M.V., 2018. Potential medium-term impacts of climate change on tuna and billfish in the Gulf of Mexico: a qualitative framework for management and conservation. *Mar. Environ. Res.* 141, 1–11.
- Domingues, R., Goni, G., Bringas, F., Muhling, B., Lindo-Atichati, D., Walter, J., 2016. Variability of preferred environmental conditions for Atlantic bluefin tuna (*Thunnus thynnus*) larvae in the Gulf of Mexico during 1993–2011. *Fish. Oceanogr.* 25, 320–336.
- Fromentin, J.M., Powers, J.E., 2005. Atlantic bluefin tuna: population dynamics, ecology, fisheries and management. *Fish. Fish.* 6, 281–306.
- García, A., Cortes, D., Quintanilla, J., Ramirez, T., Quintanilla, L., Rodriguez, J.M., Alemany, F., 2013. Climate induced environmental conditions influencing interannual variability of Mediterranean bluefin (*Thunnus thynnus*) larval growth. *Fish. Oceanogr.* 22, 273–287.
- Gove, J.M., Whitney, J., McManus, M., Lecky, J., Carvalho, F., Lynch, J.M., Li, J., Neubauer, P., Smith, K.A., Phipps, J.E., Kobayashi, D.R., Balagso, K.B., Contreras, E. A., Manuel, M.E., Merrifield, M.A., Polovina, J.J., Asner, G.P., Maynard, J.A., Williams, G.J., 2019. Prey-sized plastics are invading larval fish nurseries. *Proc. Nat. Acad. Sci. USA* 116, 24143–24149.
- Govoni, J.J., Grimes, C.B., 1992. The surface accumulation of larval fishes by hydrodynamic convergence within the Mississippi River plume front. *Cont. Shelf Res.* 12, 1265–1276.
- Greer, A.T., Boyette, A.D., Cruz, V.J., Cambazoglu, M.K., Dzwonkowski, B., Chiaverano, L.M., Dykstra, S.L., Briseno-Avena, C., Cowen, R.K., Wiggert, J.D., 2020. Contrasting fine-scale distributional patterns of zooplankton driver by the formation of a diatom-dominated thin layer. *Limnol. Oceanogr.* 1–23.
- Grüss, A., Drexler, M., Ainsworth, C.H., 2014. Using delta generalized additive models to produce distribution maps for spatially explicit ecosystem models. *Fish. Res.* 159, 11–24.
- Habtes, S., Müller-Karger, F.E., Roffer, M., Lamkin, J.T., Muhling, B., 2014. A comparison of sampling methods for larvae of medium and large epipelagic fish species during spring SEAMAP ichthyoplankton surveys in the Gulf of Mexico. *Limnol. Oceanogr. Meth.* 12, 86–101.
- Hare, J.A., 2014. The future of fisheries oceanography lies in the pursuit of multiple hypotheses. *ICES J. Mar. Sci.* 71, 2343–2356.
- Hazen, E.L., Carlisle, A.B., Wilson, S.G., Ganong, J.E., Castleton, M.R., Schallert, R.J., Stokesbury, M.J.W., Borgrad, S.J., Block, B.A., 2016. Quantifying overlap between the deepwater horizon oil spill and predicted bluefin tuna spawning habitat in the Gulf of Mexico. *Sci. Rep.* 6, 33824.
- Hernández, C.M., Witting, J., Willis, C., Thorrold, S.R., Llopiz, J.K., Rotjan, R.D., 2019. Evidence and patterns of tuna spawning inside a large no-take marine protected area. *Sci. Rep. Nat.* 9, 10772.
- ICCAT, 2019. Report of the standing committee on research and statistics (SCRS). Madrid, September 30 - October 4.
- Incardona, J.P., Gardner, L.D., Linbo, T.L., Brown, T.L., Esbaugh, A.J., Mager, E.M., Stieglitz, J.D., French, B.L., Labenia, J.S., Laetz, J.S., Tagal, M., Sloan, C.A., Elizur, A., Benetti, D.D., Grosell, M., Block, B.A., Scholz, N.L., 2014. Deepwater horizon crude oil impacts the developing hearts of large predatory pelagic fish. *Proc. Nat. Acad. Sci. USA* 111, 1510–1518.
- Ingram, G.W.Jr., Richard, W.J., Lamkin, J.T., Muhling, B., 2010. Annual indices of Atlantic bluefin tuna (*Thunnus thynnus*) larvae in the Gulf of Mexico developed using delta-lognormal and multivariate models. *Aquat. Living Resour.* 23, 35–47.
- Kim, Y.S., Delgado, D.I., Cano, I.A., Sawada, S., 2015. Effect of temperature and salinity on hatching and survival of yellowfin tuna *Thunnus albacares*. *Fish. Sci.* 81, 891–897.
- Kimura, S., Kato, Y., Kitagawa, T., Noaki, Y., 2010. Impacts of environmental variability and global warming scenario on Pacific bluefin tuna (*Thunnus orientalis*) spawning grounds and recruitment habitat. *Progr. Oceanogr.* 86, 39–44.
- Kitchens, L.L., Rooker, J.R., 2014. Habitat associations of dolphinfin larvae in the Gulf of Mexico. *Fish. Oceanogr.* 23, 460–471.
- Lang, K.L., Grimes, C.B., Shaw, R.F., 1994. Variations in the age and growth of yellowfin tuna larvae, *Thunnus albacares*, collected about the Mississippi River plume. *Environ. Biol. Fish.* 39, 259–270.
- Lehodey, P., Chai, F., Hampton, J., 2003. Modelling climate-related variability of tuna populations from a coupled ocean-biogeochemical-populations dynamics model. *Fish. Oceanogr.* 12, 483–494.
- Lehodey, P., Alheit, J., Barange, M., Baumgartner, T., Beaugrand, G., Drinkwater, K., Fromentin, J.M., Hare, S.R., Ottersen, G., Perry, R.I., Roy, C., van der Linden, C.D., Werner, F., 2006. Climate variability, fish, and fisheries. *Am. Meteorol. Soc.* 19, 5009–5030.
- Leroux, S.J., 2018. On the prevalence of uninformative parameters in statistical models applying model selection in applied ecology. *PLoS One* 14 (2), e0206711.
- Lindo-Atichati, D., Bringas, F., Gon, G., Muhling, B., Müller-Karger, F.E., Habtes, S., 2012. Varying mesoscale structures influence larval fish distribution in the northern Gulf of Mexico. *Mar. Ecol. Progr. Ser.* 463, 245–257.
- Llopiz, J.K., Hobday, A.J., 2015. A global comparative analysis of the feeding dynamics and environmental conditions of larval tunas, mackerels, and billfishes. *Deep Sea Res. Part II Top. Stud. Oceanogr.* 113, 113–124.
- Llopiz, J.K., Richardson, D., Shiroza, A., Smith, S., Cowen, R., 2010. Distinctions in the diets and distributions of larval tunas and the important role of appendicularians. *Limnol. Oceanogr.* 55, 983–996.
- Malca, E., Muhling, B., Franks, J., García, A., Tilleye, J., Gerard, T., Ingram, W., Lamkin, J.T., 2017. The first larval age and growth curve for bluefin tuna (*Thunnus thynnus*) from the Gulf of Mexico: comparisons to the straits of Florida, and the Balearic Sea (Mediterranean). *Fish. Res.* 190, 24–33.
- Maunder, M.N., Piner, K.R., 2014. Contemporary fisheries stock assessment: many issues still remain. *ICES J. Mar. Sci.* 72, 7–18.
- Mourato, B.L., Hazin, F., Bigelow, K., Musyl, M., Carvalho, F., Hazin, H., 2014. Spatio-temporal trends of sailfish, *Istiophorus platypterus* catch rates in relation to spawning ground and environmental factors in the equatorial and southwestern Atlantic Ocean. *Fish. Oceanogr.* 23, 32–44.
- Muhling, B., Lamkin, J.T., Roffer, M.A., 2010. Predicting the occurrence of Atlantic bluefin tuna (*Thunnus thynnus*) larvae in the northern Gulf of Mexico: building a classification model from archival data. *Fish. Oceanogr.* 19, 526–539.
- Muhling, B.A., Lee, S.K., Lamkin, J.T., 2011. Predicting the effects of climate change on bluefin tuna (*Thunnus thynnus*) spawning habitat in the Gulf of Mexico. *ICES J. Mar. Sci.* 68, 1051–1062.
- Muhling, B.A., Roffer, M.A., Lamkin, J.T., Ingram Jr., G.W., Upton, M.A., Gawlikowski, G., Muller-Karger, F., Habtes, S., Richards, W.J., 2012. Overlap between Atlantic bluefin tuna spawning grounds and observed deepwater horizon surface oil in the northern Gulf of Mexico. *Mar. Pollut. Bull.* 64, 679–687.
- Pearce, J., Ferrier, S., 2000. Evaluating the predictive performance of habitat models developed using logistic regression. *Ecol. Model.* 133, 225–245.

- Pepin, P., 1991. Effect of temperature and size on development, mortality, and survival rates of the pelagic early life history stages of marine fish. *Can. J. Fish. Aquat. Sci.* 48, 503–518.
- Potts, J.M., Elith, J., 2006. Comparing species abundance models. *Ecology* 99, 153–163.
- Puncher, G.N., Arrizabalaga, H., Alemany, F., Cariani, A., Oray, I.K., Karakulak, F.S., Basilone, G., Cuttitta, A., Mazzola, S., Tinti, F., 2015. Molecular identification of Atlantic Bluefin tuna (*Thunnus thynnus*, Scombridae) larvae and development of a DNA character-based identification key for Mediterranean scombrids. *PLoS One* 10, 1–19.
- Quian, H., Li, Y., He, R., Eggleston, D.B., 2015. Connectivity in the intra-American seas and implications for potential larval transport. *Coral Reefs* 34, 403–417.
- R Development Core Team, 2017. *R: A Language and Environment for Statistical Computing*. R Foundation for Statistical Computing, Vienna, Austria. www.R-project.org.
- Randall, L.L., Smith, B.L., Cowan, J.H., Rooker, J.R., 2015. Habitat characteristics of bluntnose flyingfish *Prognichthys occidentalis* (Actinopterygii, Exocoetidae), across mesoscale features in the Gulf of Mexico. *Hydrobiologia* 749, 97–111.
- Reglero, P., Urtizberea, A., Torres, A.P., Alemany, F., Fiksen, Ø., 2011. Cannibalism among size classes of larvae may be a substantial mortality component in tuna. *Mar. Ecol. Prog. Ser.* 433, 205–219.
- Reglero, P., Tittensor, D.P., Álvarez-Berastegui, D., Aparicio-González, A., Worm, B., 2014. Worldwide distributions of tuna larvae: revisiting hypotheses on environmental requirements for spawning habitats. *Mar. Ecol. Prog. Ser.* 501, 207–224.
- Reglero, P., Ortega, A., Balbín, R., Abascal, F.J., Medina, A., Blanco, E., de la Gándara, F., Álvarez-Berastegui, D., Hidalgo, M., Rasmuson, L., Alemany, F., Fiksen, Ø., 2018. Atlantic bluefin tuna spawn at suboptimal temperatures for their offspring. *Proc. R. Soc. B* 285, 20171405.
- Richards, S.A., 2005. Testing ecological theory using the information theoretic approach: examples and cautionary results. *Ecology* 86, 2805–2814.
- Richards, W.J., 2006. Scombridae: mackerels and tunas. In: Richards, W.J. (Ed.), *Early stages of Atlantic fishes: an identification guide for the western central North Atlantic*, pp. 2187–2227. Boca Raton.
- Richards, W.J., Potthoff, T., Kim, J., 1990. Problems identifying tuna larvae species (Pisces: Scombridae: *Thunnus*) from the Gulf of Mexico. *Fish. Bull.* 88, 607–609.
- Richardson, D.E., Llopiz, J.K., Guigand, C.M., Cowen, R.K., 2010. Larval assemblages of large and medium-sized pelagic species in the straits of Florida. *Prog. Oceanogr.* 86, 8–20.
- Roberts, J.J., Best, B.D., Dunn, D.C., Trembl, E.A., Halpin, P.N., 2010. Marine geospatial ecology tools: an integrated framework for ecological geoprocessing with ArcGIS, Python, R, MATLAB, and C++. *Environ. Modell. Soft.* 25, 1197–1207.
- Robin, X., Turck, N., Hainard, A., Tiberti, N., Lisacek, F., Sanchez, J.-C., Müller, M., 2011. pROC: an open-source package for R and S+ to analyze and compare ROC curves. *BMC Bioinform.* 12, 77.
- Rooker, J.R., Simms, J.R., Wells, R.J.D., Holt, S.A., Holt, G.J., Graves, J.E., Furey, N.B., 2012. Distribution and habitat associations of billfish and swordfish larvae across mesoscale features in the Gulf of Mexico. *PLoS One* 7, e34180.
- Rooker, J.R., Kitchens, L.L., Dance, M.A., Wells, R.D., Falterman, B., Cornic, M., 2013. Spatial, temporal, and habitat-related variation in abundance of pelagic fishes in the Gulf of Mexico: potential implications of the deepwater horizon oil spill. *PLoS One* 8, e76080.
- Satoh, K., Tanaka, Y., Masujima, M., Okazaki, M., Kato, Y., Shono, H., Suzuki, K., 2013. Relationship between the growth and survival of larval Pacific bluefin tuna, *Thunnus orientalis*. *Mar. Biol.* 160, 691–702.
- Schmid, M.S., Cowen, R.K., Robinson, K., Luo, J.Y., Briseño-Avena, C., Sponaugle, S., 2020. Prey and predator overlap at the edge of a mesoscale eddy: fine-scale, in-situ distributions to inform our understanding of oceanographic processes. *Nat. Scient. Rep.* 10–921.
- Skern-Mauritzen, M., Ottersen, G., Handegard, N.O., Huse, G., Dingsør, G.E., Stenseth, N. C., Kjesbu, O.S., 2016. Ecosystem processes are rarely included in tactical fisheries management. *Fish. Fish.* 17, 165–175.
- Wexler, J.B., Margulies, D., Scholey, V.P., 2011. Temperature and dissolved oxygen requirements for survival of yellowfin tuna, *Thunnus albacares*, larvae. *J. Exp. Mar. Biol. Ecol.* 404, 63–72.
- Wobbrock, J.O., Findlater, L., Gergle, D., Higgins, J.J., 2011. The aligned rank transform for nonparametric factorial analyses using only ANOVA procedures. In: *Proceedings of the ACM Conference on Human Factors in Computing Systems (CHI '11)*. Vancouver, British Columbia (May 7–12, 2011). ACM Press, New York, pp. 143–146.
- Wood, S., 2015. *Mgcv: Mixed GAM Computation Vehicle with GCV/AIC/REML Smoothness Estimation*. R package version 1.